arXiv:cond-mat/0403226v1 [cond-mat.mtrl-sci] 9 Mar 2004

The Structure and Stokes Shift of Hydrogenated Silicon Nanoclusters

Lucas Wagner[1], Aaron Puzder[2], Andrew Williamson[2], Zachary Helms[1], Jeffrey C. Grossman[2], Lubos Mitas[1], Giulia Galli[2] and Munir Nayfeh[3]

[1]*Department of Physics, North Carolina State University, Raleigh, NC 27695-8202*

[2] *Lawrence Livermore National Laboratory, Livermore, CA 94550*

and

[3]*Department of Physics, University of Illinois at Urbana-Champaign, Urbana, IL 61801*

(Dated: February 2, 2008)

Abstract

We evaluate the optical gap and Stokes shift of several candidate 1 nm silicon nanocrystal structures using density functional and quantum Monte Carlo (QMC) methods. We find that the combination of absorption gap calculations and Stokes shift calculations may be used to determine structures. We find that although absorption gaps calculated within B3LYP and QMC agree for spherical, completely hydrogenated silicon nanocrystals, they disagree in clusters with different surface bonding networks. The nature of the Stokes shift of the ultrabright luminescence is examined by comparing possible relaxation mechanisms. We find that the exciton which reproduces the experimental value of the Stokes shift is most likely a state formed by a collective structural relaxation distributed over the entire cluster.

PACS numbers: PACS: 78.67.-n, 73.22.-f, 78.55.-m

I. INTRODUCTION

The investigation of semiconducting nanoclusters is one of the most promising directions in the search for new materials to construct optical and electronic devices, new laser materials, and biological markers[1,2,3]. The properties of nanosize clusters are typically very different from their parent bulk compounds; for example, surface passivated silicon nanoclusters show a number of interesting effects such as ultrabright luminescence[4,5,6,7,8,9] and nonlinear optical effects[10], whereas crystalline bulk silicon is optically uninteresting because of its small and indirect gap. Previous theoretical studies have employed various methods to model and understand the basic structural and electronic properties of nanosize clusters such as tight-binding[11], empirical pseudopotentials[12], density functional theory (DFT)[13,14], GW-Bethe Salpeter (GW-BSE)[15,16], and quantum Monte Carlo (QMC)[17]. Despite the significant progress that has been made, especially in interpreting the properties of larger clusters ($>$ 2 nm , $>$ 500 atoms), many open questions still exist as to how new physical effects begin to dominate the electronic structure of these clusters as the surface to volume ratio increases. These effects include the possibility of surface states, reconstructions, and impurities.

Recent optical measurements of silicon nanocrystals synthesized in macroscopic quantities using a process of first etching and then sonically breaking up a silicon wafer[18] appear to have predominantly spherical shapes, show ultrabright luminescence, and are produced in remarkably uniform batches. The smallest silicon nanoclusters in the range of 1 to 1.2 nm[18] synthesized through this method exhibit significantly different properties compared with predictions from previous studies such as smaller absorption gaps and different red shifted emission peaks (i.e. the Stokes shift)[11,12,19,20,21,22,23]. Understanding the differences in these two characteristics call for high quality electronic structure calculations which can precisely describe the effects of electron correlation in ground and excited states, charge transfers, and different surface bonding networks.

In this article, we present a state-of-the-art computational study of $\sim$ 1 nm hydrogenated Si nanocluster prototype systems in order to understand the interplay between their electronic and optical properties, their surface states and structures, and to interpret their absorption and emission processes. We employ a combination of high accuracy *ab initio* methods including DFT (using the local density approximation (LDA) and the Perdew

Burke Ernzerhof (PBE)[24] and B3LYP flavors of the generalized gradient approximation (GGA)) and QMC to elucidate the electronic and structural properties of the most relevant structural prototypes. We focus on systems with 50 to 70 total atoms which are consistent with the observed sizes that emit in the blue or at the UV edge ($\sim$ 2.90 eV). We find that surface dimerization is considered as the best possible mechanism for the occurrence of smaller gaps and Stokes shifts than would otherwise be expected in this size range[25]. We use our derived models to study the structural and electronic effects related to the observed Stokes shift, namely the energy difference between absorbed and emitted photons and the character of the corresponding exciton state. The high accuracy of our QMC calculations enables us to deduce that the mechanism most likely to be responsible for the Stokes shift in these systems is due to *a global relaxation of the cluster* rather than the stretch mode of a single surface dimer[23]. Our results demonstrate that the accurate calculation of a combination of properties is critical for a full understanding of surface reconstructions, doping, and the Stokes shift of nanoclusters in this size range. Finally, we find that despite its agreement in determining optical gaps for spherical silicon nanocrystals, B3LYP compares less favorably with QMC results for systems with reconstructed surfaces or with oxygenated surfaces.

II. CALCULATIONAL METHODS

To construct structural prototypes, we start from the bulk silicon lattice and choose a spherical region as this has the smallest surface area for a given number of atoms. The dangling bonds on the surface are saturated with hydrogen and the terminated Si atoms are classified into -SiH, -SiH_2 and -SiH_3 types. The structures with -SiH_3 are discarded as they are energetically less favorable and therefore prone to reactions with the environment. Considering prototypes with -SiH and -SiH_2 terminations in the 1-1.2 nm size regime leads to two likely ideal structures, $Si_{29}H_{36}$ and $Si_{35}H_{36}$ (Fig. 1). In some cases, DFT calculations using a planewave basis and norm-conserving pseudopotentials[26] are used to establish the equilibrium geometries and the electronic structure of these systems with a kinetic energy cutoff of 35 Ry, a Gianozzi pseudopotential for hydrogen[27], and a Hamann pseudopotential for all other atoms[28]. In other cases, Gaussian all-electron calculations using a 6-311G* basis is used[29]. As we have previously observed[17], the relaxed structures are very similar when

calculated using either LDA or gradient corrected (PBE) functionals and are fairly close to the original bulk derived structures with small adjustments of the bond lengths and angles, predominantly of the surface atoms. For each cluster, the highest occupied molecular orbital (HOMO)/ lowest unoccupied molecular orbital (LUMO) gap is calculated using LDA, PBE, and the B3LYP functional.

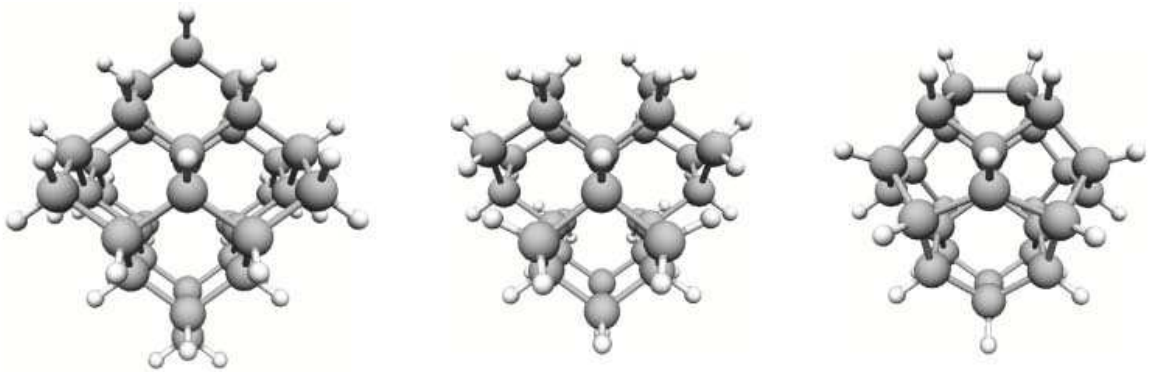


FIG. 1: Atomic structures of $Si_{35}H_{36}$, $Si_{29}H_{36}$, and $Si_{29}H_{24}$ nanocrystals. The larger spheres represent Si atoms while the smaller ones the hydrogens. Note the surface reconstruction of the top dimer from $Si_{29}H_{36}$ to $Si_{29}H_{24}$.

Although DFT techniques produce accurate minimum energy structures of silicon nanoclusters and also reliably predict the trends in the optical gap of a given structural type as a function of size[17], a more accurate approach, for example, QMC which takes many-body effects into account is required to predict the difference in optical gaps between different classes of structural prototypes, such as clusters with different surface passivants, clusters with reconstructed surfaces, or clusters with amorphous-like geometries. In addition to the computed DFT gaps, we therefore adopt a previously described QMC procedure[30,31] to perform QMC calculations using the CASINO code[32] for the optical gaps discussed in this paper.

III. PREDICTED STRUCTURE THROUGH COMPARISON WITH ABSORPTION GAP

The smallest experimentally measured clusters are determined to be $\sim$ 1 nm in diameter[18]. 1 nm clusters are too small to observe crystallinity using transmission electron microscopy (TEM), so the structure must be discerned from other experimental methods,

or deduced from physical properties such as the absorption gap and the Stokes shift. Indeed, even if TEM or other methods were capable of resolving the crystallinity of 1 nm clusters, it could not predict the surface chemistry. In a previous work, we compared the absorption gap of 1 nm spherical silicon nanoclusters with two types of reconstructed surfaces[25]. Amongst the various structures analyzed, only clusters with reconstructed dimers yielded results consistent with the experimentally measured gaps. However, in addition to all possible oxygenated clusters which were not considered, a recent molecular dynamics calculation predicted that amorphous-like 1 nm clusters can have similar gaps to those with reconstructed dimers[33]. Here, we have recalculated the gaps of these ideal and reconstructed clusters, now using linear scaling QMC[30,32] which has allowed us to obtain much smaller statistical errors, and compared them with the double cored clusters[33] as well as various oxygenated clusters. For comparison, we also compute all relevant HOMO/LUMO gaps within DFT using various functionals, focusing on the B3LYP functional in order to make a more complete comparison of this functional with computationally demanding many-body QMC results.

Table 1 shows that the optical absorption gaps as calculated within QMC of two completely hydrogenated spherical crystalline nanoclusters about 1 nm in diameter, $Si_{29}H_{36}$ and $Si_{35}H_{36}$ (5.3 and 4.9 eV) are larger than our experimentally measured value of $\sim$ 3.5 eV[18], while the crystalline cluster with reconstructed dimers are in agreement with experiment as previously shown[25]. A comparison with oxygenated clusters indicates that those with bridged oxygen are significantly higher than our experimental gaps, while those with double bonded oxygen are significantly lower, in both cases differing by over 1 eV. However, these gaps are consistent with the calculated gaps of double core amorphous-like clusters[33], suggesting both structures should be analyzed further.

In order to better understand the possibility of (2×1) dimer reconstructions, we consider here the thermodynamics of the reconstruction. While the kinetics of such a reconstruction are beyond the scope of this paper, to demonstrate that a (2×1) reconstruction is possible, we compared the total energies of the "reaction" $Si_{29}H_{36} \rightarrow Si_{29}H_{34} + H_2$. We found that within GGA methods, the balance is $\sim$ -0.3 eV (endothermic at T=0) and therefore such a dimerization may well occur for suitable chemical potentials of hydrogen. Since the preparation of the nanocrystals is performed in a mixture of HF and H_2O_2, and indeed the presence of the peroxide is crucial for obtaining the spherical shapes and nearly uniform

	LDA	B3LYP	QMC
$Si_{29}H_{36}$	3.6	5.2	5.3(1)
$Si_{35}H_{36}$	3.4	5.1	5.0(1)
$Si_{29}H_{24}$	2.6	4.0	3.5(1)
$Si_{30}H_{22}$	2.2	( )	3.1(1)
$Si_{29}H_{34}O$	3.1	4.8	4.7(1)
$Si_{35}H_{34}O$	2.2	3.9	2.6(1)
$Si_{35}H_{24}O_6$	1.7	3.3	(1.7)

TABLE I: Calculated optical gaps (eV) of some prototype 1 nm clusters using three different methods. The statistical errors in the QMC values are in parenthesis.

sizes, one could also envisage the reaction $Si_{29}H_{36}+ H_2O_2 \rightarrow Si_{29}H_{34} + 2H_2O$. Since the oxygen-oxygen distance fits reasonably well with the neighboring hydrogens on the two Si atoms such a reaction suggests a short reaction path and the process is exothermic in GGA by ~ 2.7 eV. Although the presence of H_2O_2 could also induce additional oxidation reactions of the cluster, these reactions produce clusters with absorption gaps considerably smaller than those measured here when double bonded to the surface, and larger when in a bridged configuration[31].

Recently, DFT calculations with the B3LYP functional have received some attention as a relatively computationally inexpensive alternative to such many-body methods as couple cluster, GW-BSE, and QMC for determining accurate absorption gaps[20,34,35]. Table 1 shows calculated gaps of $Si_{29}H_{34}O$ with oxygen bridged to the surface, and $Si_{35}H_{34}O$ and $Si_{35}H_{24}O_6$ with oxygen double bonded to the surface using the B3LYP functional. In each case, the gaps of the clusters with double bonded oxygen are significantly lower than the observed gaps of our 1 nm clusters but in complete disagreement with recent QMC studies. Based on the B3LYP gaps, one would conclude that our clusters are passivated by multiple double bonded oxygen atoms, specifically $Si_{35}H_{24}O_6$ (3.3 eV B3LYP gap), while the QMC results indicate otherwise. Conversely, the double core structures have gaps 1 eV higher than the experimentally measured values, when calculated within B3LYP, which would tend to eliminate these clusters as candidates. Therefore, we conclude through comparison of the absorption gap with QMC values, and through simple thermodynamic considerations,

that these clusters either have (2×1) reconstructed surfaces, although they still may be amorphous, and that like other DFT functionals, B3LYP may only generate trends that are in agreement with QMC and not quantitative values.

IV. DOPING AND CONTAMINATION OF RECONSTRUCTED SILICON CLUSTERS

In the previous section, we calculated the effects of oxygen and compared with our 1 nm prototype cluster with a reconstructed surface. In this section, we consider the effect of other contaminants, dopants, and functionalizing groups bonded to the surface of these nanoclusters. We have calculated the absorption gap of reconstructed clusters with a variety of groups and once again compared the optical gaps predicted by QMC with the single-particle B3LYP gaps. In our previous study of *unreconstructed* clusters, double-bonded groups were found to reduce the gap of 1 nm clusters by as much as 2.5 eV, while single-bonded groups reduced the gap a negligible amount[17]. Therefore, the completely hydrogenated $Si_{29}H_{36}$ cluster yields a 5.3 eV gap, higher than our observed 3.5 eV gap, while clusters with double-bonded passivants yield gaps much smaller (2.0 to 2.7 eV). This supports the (2×1) reconstructed $Si_{29}H_{24}$ cluster with a gap of 3.5 eV as a likely candidate structure for our experiment[25]. To complete the picture, we now consider the additional effect of passivant groups on this reconstructed cluster, which has heretofore *not* been considered.

Table 2 shows that our calculated LDA and B3LYP single-particle gaps for a range of groups single-bonded to the surface of $Si_{29}H_{24}$. We consider common contaminants from our synthesis process (F and OH), groups typically used to dope semiconductors (NH_2 and PH_2), and groups used to functionalize the surface (CH_3 and SH). For all these groups, the reduction of the single-particle gap compared to the prototype $Si_{29}H_{24}$ cluster is minimal ($<$ 0.1 eV) similar to the small effect of single-bonded groups on unreconstructed clusters[17]. We find that this trend exists for calculations based on the LDA, PBE, and B3LYP functionals. This lack of an effect is perhaps not surprising given that the bonding network between the surface and these single bonded passivants is the same as with hydrogen. The interplay between the dimerization (the already distorted sp^3 network) and these various passivants is thus negligible demonstrating that the dominant effect on the gap of $Si_{29}H_{24}$ is the surface reconstruction, not the presence of single-bonded passivants.

Appendage Doping	LDA/PBE	B3LYP
$Si_{29}H_{23}CH_3$	2.7	3.9
$Si_{29}H_{23}NH_2$	2.6	3.9
$Si_{29}H_{23}SH$	2.5	3.7
$Si_{29}H_{23}C_4H_8SH$	2.6	3.9
$Si_{29}H_{23}OH$	2.5	3.8
$Si_{29}H_{23}F$	2.6	3.8
$Si_{29}H_{23}PH_2$	2.7	3.9
Bridge Doping		
$Si_{29}H_{24}CH_2$	2.7	4.0
$Si_{29}H_{24}NH$	2.6	3.8
$Si_{29}H_{24}S$	2.7	3.9

TABLE II: Calculated optical gaps (eV) of dopants on reconstructed clusters using various functionals within DFT either connected to one silicon atom (appendage doping) or between two atoms (bridge doping).

While the effect of single-bonded passivants is small, we found that the SH and OH groups affect the nanocrystal gap more than other single-bonded passivants yielding a 0.2 eV red shift, similar to the observed gap reduction in OH on an unreconstructed cluster[17]. In each case, the addition of the bent group tends to distort the binding geometry at the surface, be it $Si_{35}H_{35}OH$, or $Si_{29}H_{23}SH$. The addition of a longer hydrocarbon chain to the SH (C_4H_8SH), completely eliminates this red shift as now the longer hydrocarbon chain causes less distortion at the surface. Therefore, our results show that caution should be used when using single atoms to model the effect of foreign substances on the surface of silicon nanoclusters; these single atom models tend to distort the surface to a greater extent and thus overestimate the affect on the gap compared with longer chains.

Dopants may also form in a bridged configuration which may potentially lower the gap further when coupled with dimerization. Previous calculations have shown that in Si_{29} clusters, the formation of bridged oxygen is energetically favorable to double-bonded oxygen[31]. In Table 2, we compare the gaps of a number of additional dopants in an Si-X-Si

configuration with X = S, NH, and CH_2. The Si-X-Si bridge replaces a reconstructed dimer on the surface. Again, we find the effect of these bridged dopants is negligible.

These minimal shifts in the optical absorption gap mean that single-bonded and bridged contaminants cannot be distinguished from fully hydrogenated clusters in optical absorption measurements and thus may be present on our clusters. The calculation of other physical properties such as the Stokes shift are then required for additional characterization.

V. STOKES SHIFT

A. Mechanism

One of the most intriguing features of nanocrystals is the possibility of forming self-trapped excitons which are closely related to the Stokes shift. This possibility has been the subject of several recent studies using a variety of models[21,22,23,36]. In particular, Allan *et al.* have examined models involving both a relaxation mechanism involving the entire cluster[21] and more recently a model based on the assumption that, after absorption, the exciton leads to a stretching of a particular surface Si-Si dimer bond, to form a self-trapped exciton[23]. The motivation for reexamining a range of different models arises from the observation that many experiments on 1 nm clusters appear to lead to pronounced Stokes shifts. However, in our experiments we obtained values of $\sim$ 0.4 - 0.5 eV[18] which are *significantly smaller* than previously calculated $\sim$ 1-2 eV for this range of sizes[23,37]. By calculating the Stokes shift in ideal 1 nm clusters, in those with reconstructed surfaces, in those with bridged oxygen, and in double-core amorphous-like clusters, we hope to demonstrate the use of the Stokes shift as a useful characterization method.

Before comparisons of the excitations in different structural prototypes can be made, we first need to determine the appropriate relaxation mechanisms. To resolve this issue we have performed *ab initio* calculations of the relaxation of the candidate structures discussed above in both the ground and excited (excitonic) electronic states. In addition, we have used QMC calculations to provide highly accurate values for the electronic gaps of the ground and excited state structures to accurately determine the magnitude of the Stokes shift associated with each model. Since it is computationally easier to relax the electronic structure in the optically forbidden triplet excited state, we used the triplet state to carry out

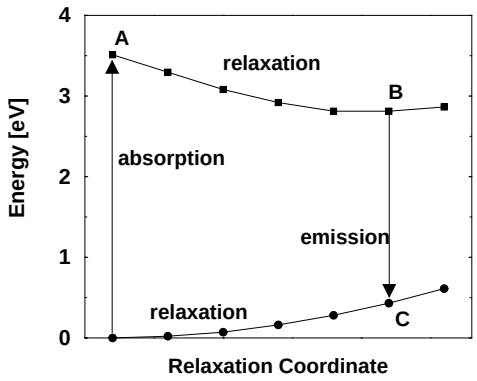


FIG. 2: Illustration of the Stokes shift in $Si_{35}H_{34}$ within the collective relaxation mechanism using energies from local density approximation calculations.

most of geometry scanning and relaxation calculations. For a few points on energy surfaces we have verified that the singlet and triplet energies were within ~ 0.03 eV. Therefore, the measured Stokes shift is about an order of magnitude larger than the singlet-triplet splitting, in direct contradiction to the model proposed by Takagahara[22] for the Stokes shift in silicon nanoclusters.

To compare different Stokes shift mechanisms, we choose to study the $Si_{29}H_{34}$ structure. This cluster has the same structure as the $Si_{29}H_{36}$ prototype, except that one of the -SiH_2 surface pairs has been reconstructed to form a dimer. By studying the Stokes shift in this cluster we are able to examine the competition between a dimer localized Stokes shift and a global relaxation of the cluster. In addition, we are able to compare with previous studies[23,38,39] of this system. In Fig. 2 we plot the LDA total energy of a $Si_{29}H_{34}$ nanocrystal in both the ground state (lower curve: circles) and excited state using the ground state structure total energy as a reference. Once the photon is absorbed (point A) the system is in the excited state and the slower ($\approx$ picoseconds) structural relaxation occurs.

The decrease in the energy from the point A to B is due to the collective relaxation of all atomic positions of the entire cluster without any constraint except that the system is in the excited electronic state. In the two symmetric clusters, either the unreconstructed $Si_{29}H_{36}$, or the $Si_{29}H_{24}$, the excitation is formed by promoting an electron from the p-like HOMO to the s-like LUMO, leading to a small distortion of the cluster from a spherical to slightly elliptical geometry. The position C corresponds to the state after photon emission and before the subsequent relaxation to the ground state. The key features which emerge

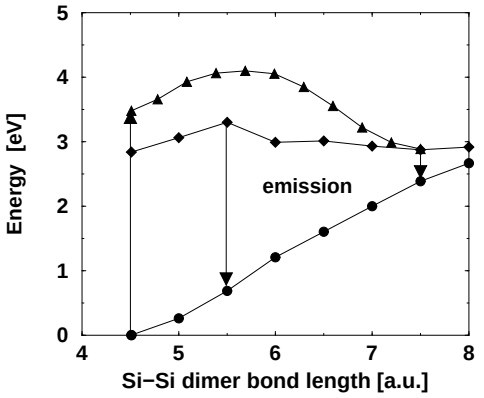


FIG. 3: Density functional Stokes shift calculations of $Si_{35}H_{34}$ within the local bond-breaking relaxation mechanism.

from our calculations are: a) barrierless relaxation to a lower energy geometry and b) small geometry adjustments of ~ 0.01 A of essentially all atoms in the cluster.

In Fig. 3 we analyzed the model of a self-trapped exciton based on a stretching and breaking of the single dimer bond, as proposed in Ref.[23]. The geometries used to generate the upper triplet curve (triangles) were obtained by linearly interpolating the atomic positions between the ground state geometry ($d_{Si-Si} = 2.4$ Å) and the local minimum energy structure obtained when d_{Si-Si} was constrained to 4.0 Å. This upper curve closely reproduces the calculation originally presented in Fig. 2 of Ref.[23] for this system, where the intermediate structures were also derived from linear interpolation. The points on the lower curve (diamonds) were obtained by constraining the dimer bond length, d, to a series of different values, while allowing all other atoms to relax while keeping the system in the excited state.

Examining Fig.3, we observe that if the system goes along the structural path leading to the broken dimer bond, it first has to overcome a barrier of ~ 0.5 eV due to the elastic energy of the cluster before the energy decreases as the bond breaks ($d_{Si-Si} > 2.9$ Å). It is interesting that the minimum energy of the excited state resulting from the global relaxation in Fig.3 is almost identical (2.8 eV) to the minimum obtained by breaking the dimer, 2.9 eV. However, the important difference is in the large energy increase on the ground state path which in turn leads to a very large Stokes shift and small energy of the emitted photon. The curve represented by interpolating the atomic coordinates between the ground state structure and the structure of a broken dimer ($d_{Si-Si} \sim 4.0$ Å) as suggested in Ref.[23] yields a markedly different energy surface to the more realistic case in which all the atoms, except

the dimer, are relaxed for each dimer length.

We have also examined the Stokes shift relaxation mechanism proposed in Ref.[39] where a hydrogen atom attached to one of two neighboring Si-H surface groups moves into a bridged position between the silicon atoms and the Si-Si bond stretches. In contrast to the semi-empirical calculations used to predict this structure[39], our density functional calculations do not find this structure to be a meta-stable state. We find a spontaneous relaxation from this proposed bridge structure to a structure in which the bridged hydrogen is completely transfered to the neighboring Si, producing an Si-H_2 group and a Si with a dangling bond. Interestingly, this structure is energetically competitive (3.1 eV above groundstate) with the relaxed excited state structures shown in Figs. 2 and 3. However, as with the dimer breaking mechanism illustrated in Fig. 3, there is a significant energy barrier between the groundstate structure and this one.

Based on these results, three different mechanisms from which a Stokes shift could result are possible. After absorbing a photon the cluster could then: i) relax via the collective structural mechanism (Fig. 2) to point (B) where the electron and hole then vertically recombine to point (C); or, ii) absorb enough energy from thermal fluctuations or higher vibronic states[40] to overcome the barrier and either break the dimer[23] or transfer a hydrogen[39] with subsequent emission and relaxation to the ground state (Fig. 3, triangles); or, iii) absorb enough energy from thermal excitations to partially stretch the dimer and to recombine from the top of the barrier. The LDA values of the Stokes shift for these three mechanisms are 1.1, 3.0 and 0.9 eV, respectively. The significantly larger Stokes shift for mechanism ii) arises mostly from the large increase in the ground state energy associated with the stretching of the dimer bond. At the minimum of the excited state, the dimer is effectively broken and the ground state energy has increased by $\sim$ 2.5 eV, the energy required to create two dangling bonds.

Given the very large Stokes shift associated with the creation of a surface dimer or transfer of hydrogen, coupled with the significant barrier that first has to be overcome before it is energetically favorable to stretch the dimer, we believe that the mechanism most likely to be responsible for the Stokes shift is the global relaxation mechanism of Fig. 3. We have therefore calculated within both DFT (LDA and GGA) and QMC the values of the total energies at points A to C for the three candidate structures.

B. Results

The QMC values for the Stokes shifts (Table 3), defined as $(E_A - E_{\text{ground}}) - (E_B - E_C)$, for $Si_{29}H_{36}$, $Si_{29}H_{24}$ and $Si_{35}H_{36}$ are 1.1, 0.42 and 0.8 eV, respectively, and agree well with those predicted by LDA and PBE which are about 0.1 eV higher in each case. While the decrease in value between the $Si_{29}H_{36}$ and the $Si_{35}H_{36}$ cluster demonstrates clearly the size dependence of ideal spherical silicon nanoclusters, the QMC value of $Si_{29}H_{24}$ is in closest agreement with the measured value of ~ 0.45 eV[9]. Therefore, when combined with our estimation for the gap, $Si_{29}H_{24}$ remains a realistic prototype for both the structure and excited states processes observed in our experiments.

	Stokes Shift	
	LDA	QMC
$Si_{29}H_{36}$	1.1	1.0
$Si_{35}H_{36}$	0.8	0.7
$Si_{29}H_{24}$	0.5	0.45
$Si_{30}H_{22}$	3.0	

TABLE III: Calculated Stokes shifts (eV) of some prototype 1 nm clusters calculated within LDA and QMC. The large shift in $Si_{30}H_{22}$ renders the QMC unnecessary.

We also consider here the non-crystalline 1 nm clusters which have been predicted to form during chemical vapor deposition at high temperatures by quantum molecular dynamics (QMD) simulations[33]. Although not applicable to the sonification process demonstrated here, these non-crystalline clusters were shown to have a gap comparable to those with ideal reconstructed clusters. We calculate the Stokes shift of these clusters to ascertain whether they have the 0.4 to 0.5 eV Stokes shifts observed in our clusters and predicted for reconstructed clusters. Surprisingly, we find very large Stokes shifts, on the order of the gap size! These non-crystalline 1 nm clusters behave more like small molecules[41] than quantum dots. Thus, the Stokes shift has proved a very powerful characterization technique eliminating the "double core" non-crystalline clusters as being those observed here.

VI. CONCLUSION

In conclusion, we have carried out a thorough study of hydrogen terminated silicon nanoclusters in the 1 - 1.2 nm range. We investigated several prototype structures and compared their optical absorption gaps and Stokes shifts with recent measurements and found that although a few other structures may yield a similar gap, most notably an amorphous-like double core cluster, only $Si_{29}H_{24}$ yields both the correct gap and Stokes shift. Thus, we determine that *both* properties must be considered when evaluating candidate structures to interpret optical measurements. We determined that B3LYP generates inconsistent results for clusters with localized orbitals compared with QMC level calculations. The atomistic first-principles DFT approaches coupled with QMC allowed us to study the optically induced excitons and to conclude that the most likely mechanism causing the Stokes shift is the barrierless relaxation of the whole structure with the red shift of ~ 0.4 eV in agreement with experiment. Comparison with further experimental data indicates that the $Si_{29}H_{24}$ structural prototype is the most promising candidate of the possibilities we tested. We have also investigated the effect of doping with a number of atoms and molecular groups. Like ideal unreconstructed structures, sp^3 bonded passivants have a minimal effect on absorption gaps, as do single bridged passivants. Therefore, other atoms or ligands may be used to functionalize these clusters with no discernible change to the gap.

We thank Erik Draeger for providing QMD non-crystalline structures and for helpful discussions. In part this work was performed under the auspices of the U.S. Department of Energy by the University of California, Lawrence Livermore National Laboratory under contract No. W-7405-Eng-48. We also gratefully acknowledge NSF support from the grant DMR-0102668 and M.N. acknowledges support by the NSF grant. Part of the calculations has been done at NCSA, University of Illinois.

---

[1] A. D. Yoffe, Adv. Phys. **50**, 1 (2001) and references therein.

[2] C.C. Chen, A.B. Herhold, C.S. Johnson, and A.P. Alivisatos, Science **276**, 398 (1997).

[3] W.C.W. Chan and S. Nie, Science **281**, 2016 (1998).

[4] S. Furukawa and T. Miyasato, Phys. Rev. B **38**, 5726 (1998).

[5] W. L. Wilson, P.F. Szajowski, and L.E. Brus, Science **262**, 1242 (1993).

[6] S. Schuppler, S.L. Friedman, M.A. Marcus, D.L. Adler, Y.H. Xie, F.M. Ross, T.D. Harris, W.L. Brown, Y.J. Chabal, L.E. Brus, and P.H. Citron, Phys. Rev. Lett. **72**, 2648 (1994).

[7] T. van Buuren, L.N. Dinh, L.L. Chase, W.J. Siekhaus, and L.J. Terminello, Phys. Rev. Lett. **80**, 3803 (1998).

[8] J.D. Holmes, K.J. Ziegler, R.C. Doty, L.C. Pell, K.P. Johnston, and B.A. Korgel, J. Am. Chem. Soc. **123**, 3743 (2001).

[9] G. Belomoin, J. Therrien, A. Smith, S. Rao, R. Twesten, S. Chaieb, M.H. Nayfeh, L. Wagner, and L. Mitas, Appl. Phys. Lett. **80**, 841 (2002).

[10] M. H. Nayfeh, N. Barry, J. Therrien, O. Akcakir, E. Gratton, and G. Belomoin, Appl. Phys. Lett. **78**, 1131 (2001).

[11] J. P. Proot, C. Delerue and G. Allan, Appl. Phys. Lett. **61**, 1948 (1992).

[12] L.-W. Wang and Alex Zunger, J. Chem. Phys. 100, 2394 (1994).

[13] B. Delley and E.F. Steigmeier, Phys. Rev. B **47**, 1397 (1993).

[14] S. Ogut, J. R. Chelikowsky and S. G. Louie, Phys. Rev. Lett. **79**, 1770 (1997).

[15] M. Rohlfing and S. G. Louie, Phys. Rev. Lett. **80**, 3320 (1998).

[16] L.X. Bendict, A. Puzder, A.J. Williamson, J.C. Grossman, G. Galli, J.E. Klepeis, J.-Y. Raty, and O. Pankratov, Phys. Rev. B **68**, 085310 (2003).

[17] A. Puzder, A. J. Williamson, J.C. Grossman, and Giulia Galli, Phys. Rev. Lett. **88**, 097401 (2002).

[18] G. Belomoin, J. Therrien, and M.H. Nayfeh, Appl. Phys. Lett. **77**, 779 (2000).

[19] I. Vasiliev, S. Ogut, J.R. Chelikowsky, Phys. Rev. Lett. **86**, 1813 (2001).

[20] A.J. Williamson, J.C. Grossman, R.Q. Hood, A. Puzder, and G. Galli, Phys. Rev. Lett. **89**, 196803 (2002).

[21] E. Martin, C. Delerue, G. Allan, and M. Lannoo Phys. Rev. B **50**, 18258 (1994).

[22] T. Takagahara and K. Takeda, Phys. Rev. B **53**, R4205 (1996).

[23] G. Allan, C. Delerue and M. Lannoo, Phys. Rev. Lett. **76**, 2961 (1996).

[24] J.P. Perdew, K. Burke, and M. Ernzerhoff, Phys. Rev. Lett. **78**, 1396 (1997).

[25] L. Mitas, J. Therrien, R. Twesten, G. Belomoin, and M.H. Nayfeh, Appl. Phys. Lett. **78**, 1918 (2001).

[26] The code GP 1.8.0 (F.Gygi, LLNL) was used.

[27] P. Gianozzi (Private Communication).

[28] D. Hamann Phys. Rev. B, **40**, 2980 (1989).

[29] M.J. Frisch *et al.*, A.4 ed., Gaussian, Inc., Pittsburgh, PA (1998).

[30] A.J. Williamson, Randolph Q. Hood and J. C. Grossman, Phys. Rev. Lett. **87**, 246406 (2001).

[31] A. Puzder, A.J. Williamson, J.C. Grossman, and G. Galli, J. Chem. Phys. **117** 6721 (2002).

[32] R. J. Needs, G. Rajagopal, M. D. Towler, P. R. C. Kent and A. J. Williamson, CASINO version 1.0 User's Manual, University of Cambridge, Cambridge 2000.

[33] E. Draeger, J.C. Grossman, A. J. Williamson, and G. Galli, Phys. Rev. Lett. **90**, 167402 (2002).

[34] C.S. Garoufalis, A.D. Zdersis, and S. Grimme, Phys. Rev. Lett. **87**, 276402 (2001).

[35] Z. Zhou, L. Brus, and R. Friesner, Nanoletters **3**, 163 (2003).

[36] A. Puzder, A.J. Williamson, J.C. Grossman, and G. Galli, J. Am. Chem. Soc. **125** 2786 (2003).

[37] M.V. Wolkin, J. Jorne, P.M. Fauchet, G. Allan, and C. Delerue, Phys. Rev. Lett. **82**, 197 (1999).

[38] M. Hirao and T. Uda, Int. J. Quant. Chem. **52**, 1113 (1994).

[39] M.J. Caldas Physica Status Solidi b **217**, 641 (2000).

[40] M.H. Nayfeh, N. Rigakis and Z. Yamani, Phys. Rev. B **56**, 2079-2084 (1997).

[41] A. Franceschetti and S.T. Pantelides, Phys. Rev. B **68**, 033313 (2003).